Received: 8 June 2020 | Revised: 29 August 2020 | Accepted: 30 August 2020

DOI: 10.1002/ffj.3623

RESEARCH ARTICLE

WILEY

Aroma absorption in rapeseed oil using rotating packed bed

Ilya Lukin | Lukas Pietzka | Isabell Wingartz | Gerhard Schembecker

Laboratory of Plant and Process Design, Department of Biochemical and Chemical Engineering, TU Dortmund University, Dortmund, Germany

Correspondence
[1]Laboratory of Plant and Process Design, Department of Biochemical and Chemical Engineering, TU Dortmund University, Emil-Figge-Strasse 70, D-44227 Dortmund, Germany.
Email: gerhard.schembecker@tu-dortmund.de

Funding information
The author(s) received no specific funding for this work.

Abstract

An increasing consumers' call for natural aromas fuels the development of biotechnological aroma production. Although aroma fermentation is quite advantageous, especially severe product losses of volatile compounds through the bioreactor off-gas may challenge the downstream processing. The application of novel process intensification methods to overcome the common drawbacks of conventional apparatuses might be helpful on a way to commercial competitiveness of biotechnological aromas. This study explored the suitability of rotating packed bed (RPB), a rotating mass transfer enhancing machine, for the absorption of model aroma compounds in rapeseed oil. Increasing the rotation speed from 500 to 2750 rpm led to two- to threefold higher absorption efficiencies at elsewise constant conditions. Aiming for an enriched aromatic intermediate, 2.5 L of rapeseed oil was processed in a recycle for 200 minutes, and a final concentration of benzaldehyde of 0.323 ± 0.026 g/L_{oil} was achieved. Compared to packed columns, the RPB outperforms at equal packing depth or requires less packing area to deliver same efficiency. Especially, the use of custom 3D-printed spiral packing with elaborated wall film flow combined with rotation supported liquid distribution allows using absorbents with viscosities as high as 100 mPa·s at low pressure drop increase. However, small dimensions severely limit the performance of a laboratory-scale RPB as the casing contributes disproportionally to mass transfer.

KEYWORDS

absorption, natural aromas, rapeseed oil, recovery, rotating packed bed

1 | INTRODUCTION

Nowadays, aromas are an essential part of many daily used products ranging from flavoured foods and feeds through cosmetics and household applications towards pharmaceuticals.[1] Especially, the rising consumer's call for all-natural formulations and the rapid improvement in genetic tools and synthesis pathways has made the biotechnological aroma production in the past decades an alternative source of natural compounds alongside plant or animal feedstock.[2-5] Mild reaction conditions, higher regio- and enantioselectivity, hardly any toxic by-products and natural labelling of the product are some of the advantages over chemical production promising the biotechnological aromas a great future.[4,6,7] Unfortunately, the partitioning of aromas between different phases and sometimes severe losses of volatile product through the off-gas still challenges the downstream processing from fermentation broth.

Abbreviations: ACN, acetonitrile; GC-FID, gas chromatography flame ionization detector; MDEA, methyl diethanolamine; MEA, monoethanolamine; RPB, rotating packed bed; RCF, relative centrifugal force; RPM, rotations per minute; VOC, volatile organic compound; VVM, volatile organic compound.

Among several techniques applicable for the recovery of biotechnological aromas, the absorption in a rotating packed bed presents a novel approach to overcome the common drawbacks of conventional apparatuses, such as mass transfer limitations, narrow operational windows and bulky machinery.[8] The rotating packed bed came from the area of process intensification in a high gravity field and was first patented in 1981 by Ramshaw and Mallinson.[9] Since then many investigations on different types and designs of RPB have been performed, showing the positive effect of the rotation on the mass transfer and process performance for applications like distillation, adsorption, stripping, absorption, mixing and even reaction compared to conventional apparatuses summarized in different comprehensive reviews.[10-12] The central element of any RPB is an annular packing inside a circular motor-driven rotor within a static casing similar to vertically arranged basket centrifuge. Under the counter-current flow, the less dense fluid, usually gas, is fed on the outer edge of the RPB casing and flows towards the inner eye, where the more dense fluid, usually liquid, is fed through a liquid distributor and flows under the centrifugal acceleration to the outer edge of the packing. The mechanical seal of the motor shaft and the gas seal of the rotor are required to prevent the gas bypass flows. The more elaborated liquid distribution and the generation of thin films and smaller droplets are the primary reasons for increased mass transfer coefficients and mass transfer areas. The rotation leads to wider flooding limits[13] and allows achieving the same separation task in a much compacter design reducing the equipment volume by 1 to 3 orders of magnitude.[14-16] As a result, a majority of the research focuses on the replacement of large absorption columns for CO_2 capture or post-combustion gas cleaning with RPBs. Despite all the advantages, persisting scepticism towards rotating equipment and still less systematic often case-by-case design is the reason for only a few applications outside China[10,11] reported with no examples of RPB use for the recovery of fine chemicals like aromas found.

As the majority of the RPB research found deals with large-scale chemical processes, the purpose of this study was to extend the RPB application field towards small-scale processes like fermentative aroma production. The assessment of the usually reported RPB advantages of enhanced mass transfer, process flexibility, and space saving also for biotechnological processes could help to promote a broader industrial RPB employment. A further aim of this study was to investigate the suitability of the RPB application for the absorption of aromas in high viscous liquids like rapeseed oil. As a hydrophobic liquid, rapeseed oil is an excellent absorbent with high affinity and high capacity for hydrophobic aromas. Its naturalness and sustainability are additional benefits for green labelling. Besides, the use of plant oils in aroma absorption could lead to an enriched aromatic oily intermediate ready to use in final formulations, for example, in cosmetics or feeds. However, the high viscosity makes the utilization of oils in conventional packed or bubble columns challenging as it influences both the hydrodynamics and the mass transfer negatively.[17,18] Here, the increase of mass transfer by rotation and the use of customized packing in the RPB may be particularly beneficial for intensification of aroma recovery in viscous liquids at moderate pressure drop. Previously, this positive effect has been shown for CO_2 absorption in aqueous monoethanolamine (MEA) or methyl diethanolamine (MDEA) solutions with low to medium viscosity in a range of η = 1.2-15 mPa·s.[19-25] Chiang et al reported the useful impact of the RPB on the absorption of hydrophobic VOCs like xylene and toluene in silicon oil,[26] unfortunately, without any specifications on the viscosity range or the silicon oil used. So far, no reports of RPB operation with plant oils of typical viscosity range around η = 51-82 mPa·s at 20°C[27] have been presented.

In order to investigate the effect of rotation on absorption efficiency and to demonstrate RPB's flexibility dealing with differently volatile products, model compounds benzaldehyde (H^{pc} = 2.7 ± 0.3 Pa·m^3·mol^{-128}), hexanal (H^{pc} = 25.5 ± 5.2 Pa·m^3·mol^{-128}) and isopentyl acetate (H^{pc} = 41.5 ± 5.3 Pa·m^3·mol^{-128}) were absorbed in rapeseed oil (η = 63 mPa·s measured at 20°C) at two different rotation speeds. At the same time, this compound screening might also show the limits of rotation enhanced mass transfer for thermodynamically unpreferred systems. Afterwards, taking benzaldehyde as a compound for which the largest effects of the rotation enhanced mass transfer is expected due to the lowest volatility, the absorption with oil recycle was performed. The general trends and conclusions of the absorption with oil recycle, however, would be the same for all the aromas using equal machinery, packing, experimental set-up, and process parameters like rotation speed, but only the absolute absorption values caused by different volatility would differ. Aiming to enrich the absorbent with aroma, 2.5 L of rapeseed oil was also processed in recycle, and the achievable aroma concentration in the oil phase was compared with the one achievable in a packed column. The dependency of the pressure drop on the viscosity of the absorbent used was measured with water-glycerol solutions (η = 1 - 100 mPa·s at 20°C). In addition, the absorption efficiency using the spiral packing was compared to the performance of the plain machine targeting at further optimization possibilities.

A custom 3D-printed packing was designed for a laboratory-scale RPB according to the theory of MacInnes[29] on spiral channel intending to deliver thin liquid flow patterns maintaining constant fluid contact area throughout changing radius. Besides the precise control over the contact area, the closed structure of the self-aspiring Archimedean spiral helps to overcome the commonly known challenge of liquid maldistribution in porous RPB packings like wire or grid mesh.[30] The liquid is dragged inside the packing regardless of the initial destitution and forced by the centrifugal force to flow at the inside wall of the spiral channel. An additional advantage of the spiral packing is the generation of thin liquid films flowing along the walls of the spiral channel. According to commonly accepted theories on mass transfer, two-film theory[31] and penetration theory,[32] the generation of thinner films increases the mass transfer as the diffusion resistance and the diffusion time decreases. Expecting the diffusion of aroma compounds being restrained due to the high viscosity[18] of the rapeseed oil, the employment of the spiral packing in combination with a high gravity field appears a good possibility for mass transfer enhancement needed to be tested.

2 | MATERIALS AND METHODS

2.1 | Experimental set-up

The experiment was set up according to Figure 1. The stripping column mimics an aerated bioreactor and is used to load the air stream with the initially liquid aroma compound. The aroma is added to the stripping column above its aqueous solubility concentration so that during the experiment, the aqueous phase in the stripping column is always oversaturated because two liquid phases are present, a saturated aqueous aroma solution and a pure aroma compound. This procedure ensures a constant aroma loading of the air passed through the stripping column. This stream is mixed with the air passed through a humidifier column to adjust the aroma concentration. The combined air stream is fed into the RPB tangentially through the outer edge of the casing, passes the rotor containing the packing towards the inner eye, and leaves the RPB tangentially from the top cover. The rapeseed oil is fed counter currently from the liquid tank by a pump (Ismatec MCP-Z Standard, Cole-Parmer, USA) and is distributed axially at the inner radius of the packing by an open pipe liquid distributor with an inner diameter of 1/8'' without any nozzle mounted. The RPB used in this study has a casing diameter of 260 mm and a height of 128 mm made from stainless steel A240-316L. It is equipped with a perforated bowl-type rotor (Figure 2) of 180 mm outer diameter (A240-316L stainless steel) containing the 3D-printed polymer spiral packing (Figure 3) with d_i = 0.045 m inner diameter, d_o = 0.174 m outer diameter and h = 0.020 m axial height. From the design procedure, the spiral pitch angle was set to 4.5°, the channel height to 2.1 mm, and the total spiral length to 2038 mm per spiral. In total, four spiral channels were incorporated in one packing with channel entries spaced 90° apart at the inner packing radius. The packing was printed using Formlabs Standard Clear resin,[33] as the chemical system studied is not chemically aggressive. The rotor was sealed towards the casing top plate by a labyrinth sealing of 25 mm depth. The RPB could be operated at rotations up to 2750 rpm corresponding to 191 rcf at the inner or 741 rcf at the outer radius of the packing. The total gas flow rate is kept constant at $\dot{G}$ = 100 L/min representing an off-gas of a technical scale bioreactor of 100 L volume at 1 vvm gassing rate. The rapeseed oil flow rate is varied from $\dot{L}$ = 0.3-2 L/min. The temperature of the gas inlet stream is kept constant at 20 ± 0.1°C. The temperature increase at the gas outlet was measured and did not exceed 1 K.

2.2 | Analytics

For the analysis of the concentration in the liquid phase, the aroma was extracted from the rapeseed oil by acetonitrile (HiPerSolv CHROMANORM®, VWR International) from the rapeseed oil samples collected at the RPB liquid outlet. The solvent was added to 2 mL of the sample in a mass ratio of 1 g_{ACN}/g_{sample}. The extraction was performed for 1 h at ambient temperature on an overhead shaker (PTR-60, Grant Bio) at 50 rpm using 5 mL Eppendorf tube. In total, 6 extraction stages per sample were performed with fresh solvent added to each stage. After each extraction step, the samples were centrifuged in a laboratory centrifuge (Centrifuge 5415 R, Eppendorf, Germany) at 13.200 rpm (16.100 rcf) for 30 s. The solvent phase of each extraction step was transferred to a separate GC vial, and the aroma concentration was determined by GC-FID analysis (Agilent, USA) using the CP-Sil 8 CB capillary column (Agilent, USA) of 25 m length, 0.32 mm diameter and 0.12 μm film thickness. Helium was used as carrier gas at 1 mL/min, and a total of 1 μL was injected at 280°C using a split ratio of 20:1. The temperature of the oven was controlled starting at 50°C for 5 minutes, linearly increasing the temperature to 200°C at 50°C/min and holding the temperature at 200°C for another 2 minutes. The FI detector was heated to 290°C and operated at 450 mL/min air flow rate, 50 ml/min hydrogen flow rate, and 30 ml/min makeup helium flow rate. The FI detector peak area was calibrated using an external aroma standard at a known concentration in an acetonitrile matrix. The aroma concentration in each sample of every single extraction step was measured separately without any pooling of any samples. No aroma was detected in any of the analysed samples of the 6th extraction stage, and thus, the total mass of the extracted aroma and by

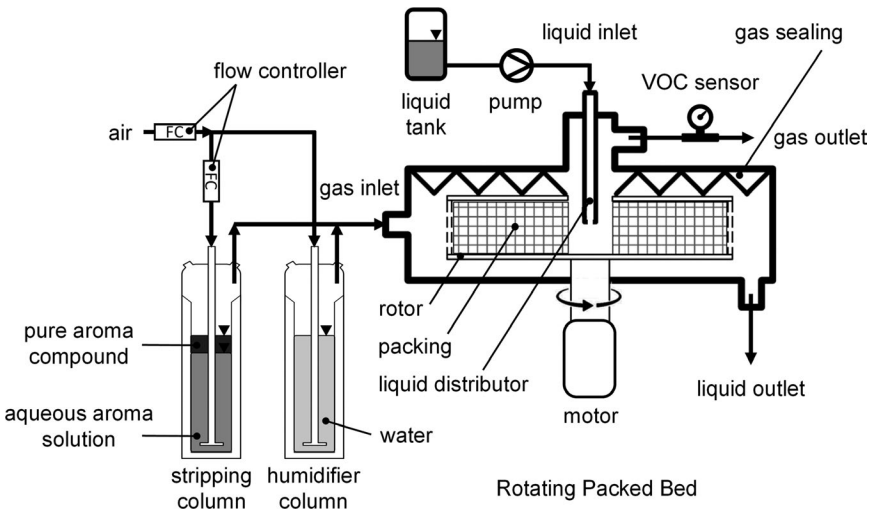

FIGURE 1 Schematic diagram of the experimental set-up for aroma absorption in an RPB

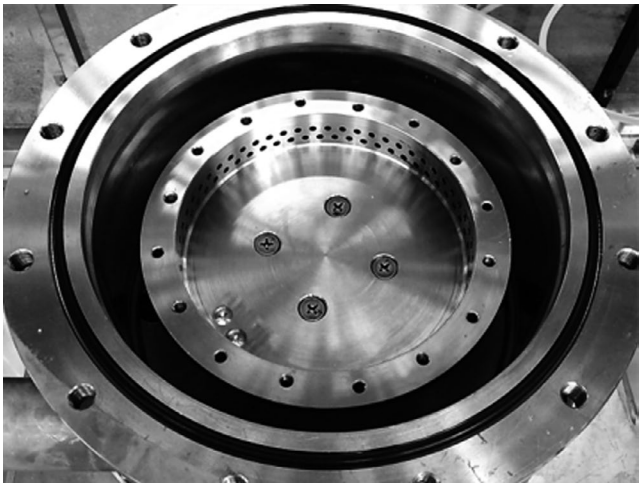

FIGURE 2 Perforated bowl-type rotor used in RPB

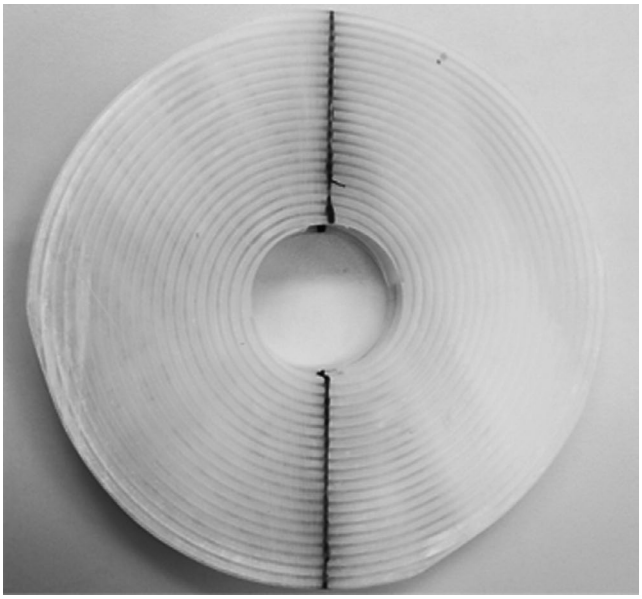

FIGURE 3 3D-printed spiral packing

that the concentration in the oil sample was recalculated from the mass balance of 5 extraction steps.

The aroma concentration in the gaseous stream was measured using a semiconductor-based mix gas sensor VOC-A-UI (ConSens GmbH) used for monitoring compartment air quality. The VOC sensor was calibrated similarly to chromatographic calibration methods injecting the known mass of a particular aroma into the stripping column at a constant gas flow rate and calculating the area under the signal-time curve generated. At the beginning of each experiment, the VOC sensor was preconditioned to the gas flow and the aroma compound at experimental parameters. After the signal of the VOC sensor for the set gas flow rate, gas temperature, aroma concentration and rotation speed of the experiment remained steady for 10 minutes, the liquid pump was turned on at the desired liquid flow rate. After a response time of the VOC sensor of 2-4 minutes, the signal steady state was reached. Therefore, each parameter set for any absorption experiment was measured for 10 minutes and the steady-state signal value of the VOC sensor was taken for the calculation of the absorption efficiency.

The absorption efficiency E was calculated from the relative differences of gaseous aroma concentration in the inlet and outlet streams Equation (1). As the VOC sensor signal is linearly proportional to the concentration of the given aroma compound (data not shown) and the system was operated with only one volatile at a time, the absorption efficiency E can be calculated directly from the VOC sensor signal difference before and during the absorption Equation (2).

$$E = \frac{c^g_{aroma,in} - c^g_{aroma,out}}{c^g_{aroma,in}} \times 100\%. \quad (1)$$

$$E = \frac{(S_{in} - S_0) - (S_{out} - S_0)}{(S_{in} - S_0)} \times 100\% \quad (2)$$

Because the VOC sensor was zeroed to a baseline value of $S_0 = 10 \pm 1\%$, the baseline is subtracted from both values. Although the VOC sensor was calibrated for every aroma used to ensure equal gas loading despite different sensor response, there is no need to recalculate the signal to concentration as the relative absorption efficiency remains the same. The absorption efficiency is one way to measure equipment's performance alongside the mass transfer coefficients. Because in the end, the absorption efficiency determines the industrial application here it is used as a more direct evaluation parameter. However, the general result trends and conclusions remain transferable to the evaluation based on mass transfer coefficients, as they are usually calculated from the measured absorption efficiency. Therefore, further assumptions of, for example, negligible resistance in the gas phase, are made, which might not be valid for semi-volatile aromas used. In this study, the absorption efficiency represents the percentage of the aroma depleted from the gaseous phase with the efficiency of 100%, meaning all aromas were absorbed, and the VOC sensor signal goes to its baseline.

In order to prove, if a significant amount of aroma is lost through the headspace of the liquid tank, the time development of liquid aroma concentration during the recycle experiments was used. The liquid aroma concentration obtained from the GC measurements was compared to the values calculated from the VOC signal based on the assumption of the closed mass balance. Under consideration of the error bars, the deviations between the two methods were not significant for any time point (no data shown). Therefore, the aroma losses can be neglected, and the measurement of gaseous aroma concentration via VOC sensor can be accepted as generally valid with the precision equal to the off-line GC measurement.

2.3 | Simulation set-up for the comparison to packed bed absorption

The experimental results of aroma absorption in RPB were compared to the performance of a packed column using a simulation

model. The simulation of well-established machinery is one way to estimate the benchmark for novel equipment like RPB without the full experimental effort of building a packed column. For the simulation of aroma absorption in packed column, ASPEN Plus 8.8 was used. A Rad-Frac module with rate-based calculation type of two stages was chosen, and both the condenser and the reboiler were disabled, and both incoming streams were fed on-stage. The column top pressure was set to 1.013 bar. The packing was defined to be MELLAPAK 350Y from SULZER to provide a comparable specific packing surface area as the packing used in RPB. The section diameter was determined starting from $d_{c,init}$ = 0.03 m corresponding to equal gas loading factor as in RPB to finally d_c = 0.06 m as a minimum to prevent column flooding. The packed section height was varied to deliver the desired comparison from H = 0.065 m corresponding to equal packing height as the radial depth of the RPB packing, over H = 0.08 m generating equal surface area as in the RPB, to H = 0.35 m providing equal performance as the RPB, finally to H = 2.9 m, delivering 90% of aroma recovery from the gaseous phase. In the packing rating section, counter-current flow with film resistances in both phases and both phases non-ideality correction was chosen because especially for semi-volatile aromas in a range of $H^{pc} = 10^0 - 10^2$ Pa·m^3·mol^{-1} both phase resistances might be important.[34] Both the mass transfer coefficient and the interfacial area were estimated using HanleyStuc (2010) correlation[35] as it is the most accurate method for structured packings such as MELLAPAK. Pure triolein, a triglyceride of oleic acid, which is contained in rapeseed oil typically at 51 - 70%,[27] up to 84%[36] was used to simulate the oil phase. The triolein incoming stream of 20°C and 1.013 bar was saturated with 0.045 mol/mol air to prevent air transfer from the gaseous phase to the oil phase during the absorption and make the results more comparable to the experimental RPB set-up. The incoming gas stream consisted of air saturated with 0.0003 mol/mol triolein and containing 25 ppm benzaldehyde. UNIFAC was chosen as a thermodynamic model for the liquid phase as it is expected to be more accurate when estimating a complex molecule like triolein consisting of glycerol and three fatty acids. Moreover, the compassion of the predicted Henry volatility coefficients in water using the extended Raoult law and activity coefficients calculated by UNIFAC delivered the lowest deviation from data collected in the literature (data not shown). Thus, the partitioning of the aroma compounds between gaseous and oily phase was determined by UNIFAC thermodynamics. No aqueous Henry's constants were manually used in the simulation. In order to simulate the recycle of the rapeseed oil and the non–steady-state enrichment of the liquid phase, in total 80 columns were connected subsequentially (Figure 4). The liquid phase was passed from column to column and contacted with the fresh gas phase of the same composition in every column as if it would have been passed 80 times through just one column. Thus, each column represents one passage of the oil through the RPB operated under liquid recycle, respectively, one absorption step. Because the rapeseed oil was passed through the RPB 80 times during the experimental investigations, in total 80 columns were needed.

2.4 | Pressure drop measurements

The pressure drop of the RPB was measured using a U-pipe manometer. The manometer was connected to the gas inlet and the gas outlet, and the pressure drop was calculated from the height difference of the water column (3).

$$\Delta p = \rho_{water} \cdot g \cdot \Delta h \tag{3}$$

The viscosity of absorbent was adjusted between 1 and 100 mPa·s by preparing water-glycerol mixtures at 20°C based on published data.[37] Each pressure drop measurement was performed two times. Because the height of the water column did not vary in an observable range between any replicates, the error bars of the

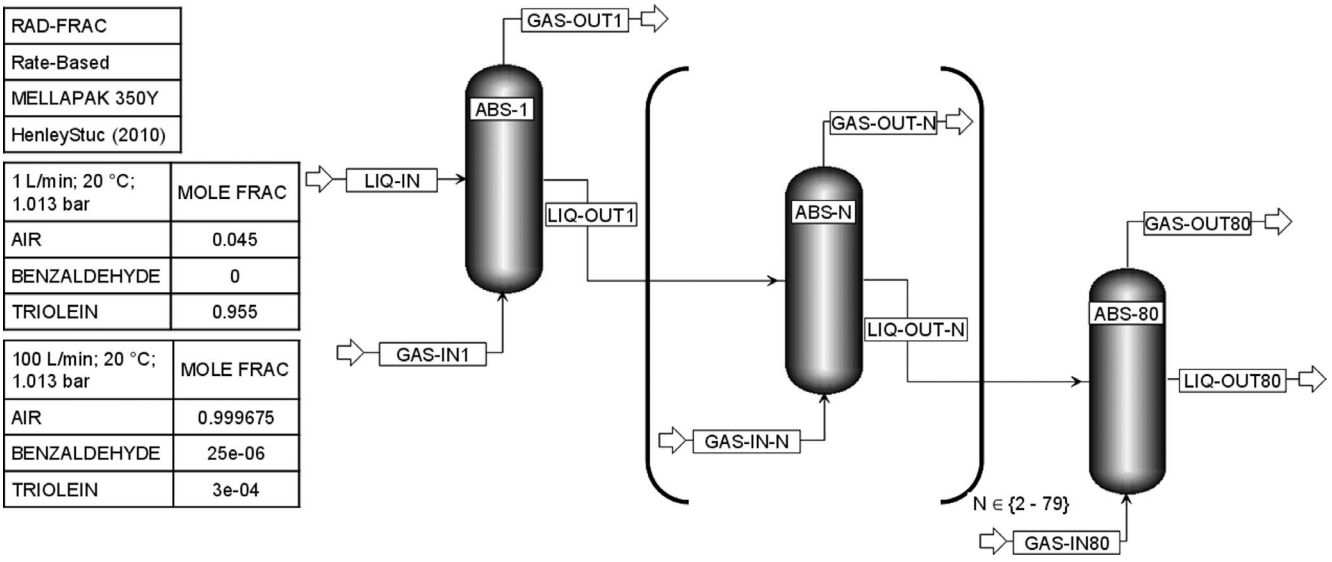

FIGURE 4 ASPEN Plus set-up for the simulation of aroma absorption in packed column with liquid recycle

pressure drop data are based on the measurement precision of ±10 Pa.

3 | RESULTS AND DISCUSSION

The aromas used in this study were selected based on the Henry coefficient H^{pc} taken from the literature for aqueous solutions allowing the classification of compounds in volatility classes. As a thermodynamic property, the Henry coefficient strongly depends on the solvent used and will differ from literature data taken in case of the rapeseed oil as an absorbent. The general classification of the volatility, however, is expected to remain in the same order with isopentyl acetate as the most and benzaldehyde as the least volatile. Thus, the Henry coefficient H^{pc} for aqueous aroma solutions is used for volatility classification in the diagrams presented despite rapeseed oil absorbent. In Figure 5, the time evolution of the gas sensor signal for these aromas is shown for two different rotation speeds.

After the start of the liquid flow, a drop in the sensor signal is observed, indicating a decreased aroma concentration in the gas outlet compared to the beginning of the experiment, meaning that a part of aroma is absorbed in oil. Steady state is reached within 2 to 3 minutes after the start of the liquid flow. However, the observations of the sensor behaviour suggest that most of the dynamics of the signal come from the slow sensor response, and the actual steady state inside the RPB is reached probably even faster. Once the rotation speed is increased from 500 rpm, corresponding to 6 rcf on the inner packing radius to 2750 rpm (191 rcf) at 15 minutes, the sensor signal decreases further, implying an enhanced absorption. From the different relative signal drops, it is evident that the absorption is the highest for benzaldehyde, followed by hexanal and isopentyl acetate. This observation is underlined in Figure 6, where the absorption efficiency is presented over Henry's volatility coefficient for the three aromas and the two rotation speeds investigated.

In agreement with the widely reported positive effect of the rotation on mass transfer, the increase of the centrifugal force leads to a two- to threefold increased absorption efficiency for all aromas. According to a common theory for mass transfer, the mass flow of a certain compound for a constant driving force (the concentration gradient Δc) depends on the mass transfer coefficient k and the mass transfer area a (4)[38]

$$\dot{n}_i = k \cdot a \cdot \Delta c_i \tag{4}$$

As the mass transfer area a in the spiral packing remains constant for all operational parameters once the full wall film is established, the absorption increase can be traced back to an increased mass transfer coefficient k. The mass transfer coefficient is a function of the binary diffusion coefficient and the thickness of the boundary layer (5).[38]

$$k = \frac{D_{AB}}{\delta} \tag{5}$$

At higher rotation speed, greater shear forces lead to the formation of thinner liquid films with faster surface renewal, decreasing the boundary layer thickness δ and by that the mass transfer resistance. In his research, Holly[39] found out that the thickness of the diffusion sublayer mainly depends on the flow and mixing conditions and is inversely proportional to the Schmidt and Reynolds numbers and thus to the fluid velocity. As the liquid flow rate and with it the liquid velocity and Schmidt and Reynolds numbers remain the same, it can be assumed that the film thickness as a hydrodynamic parameter remains equal for all three aromas as it should depend on flow conditions applied only. The binary diffusion coefficient as a thermodynamic parameter, however, depends for the constant absorbent on the aroma properties and is expected to decrease from the least volatile benzaldehyde over hexanal to the most volatile isopentyl acetate. Combined, it would lead to different mass transfer coefficients and result in the observed decreasing absorption efficiency for aromas with larger Henry coefficient.

The positive effect of the rotation supported distribution of viscous liquids can be used not only to increase the mass transfer of a particular aroma but also to process more volatile components in a multipurpose plant intensifying the use of the equipment. Going from 500 to 2750 rpm allowed the absorption of more volatile isopentyl acetate (H^{pc} = 41.5 ± 5.3 Pa·m^3·mol^{-128}) compared to benzaldehyde (H^{pc} = 2.7 ± 0.3 Pa·m^3·mol^{-128}) at constant absorption efficiency. Another possibility for further process intensification of the aroma absorption in RPB is to increase the liquid enrichment with aroma through the recycle of oil. Reusing the oil phase does not only save absorbent but is in particular beneficial when an enriched aromatic intermediate can be utilized in a final formulation without further downstream processing.

Herefore, 2.5 L of rapeseed oil is pumped through the RPB in a closed loop for nearly 3.5 h at a constant throughput of 1 L/min and constant gas inlet composition. In Figure 7, the time evolution of the gas sensor signal shows a rather slow signal increase over time after an initial drop. This slow dynamic shows that the steady state is not achieved after 80 absorption cycles yet and indicates a large capacity of rapeseed oil for benzaldehyde. The rapeseed oil is not saturated and absorbs aroma from the gaseous phase during the

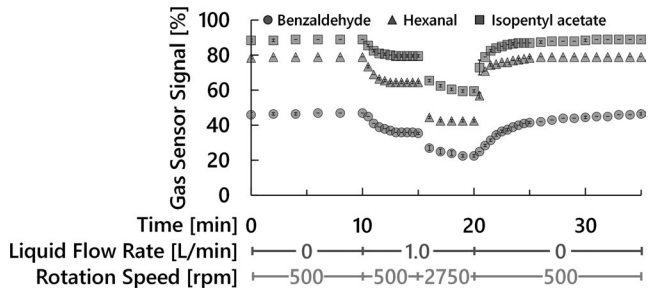

FIGURE 5 Time evolution of the gas sensor signal for the absorption for different aroma compounds in an RPB using rapeseed oil at different rotation speeds (G = 100 L/min; N = 3)

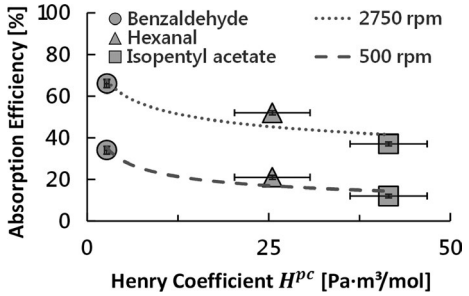

FIGURE 6 Dependency of the absorption efficiency on aroma volatility for the absorption of different aroma compounds in an RPB using rapeseed oil at different rotation speeds (G = 100 L/min, L = 1 L/min; N = 3; the lines are added to guide the eye only)

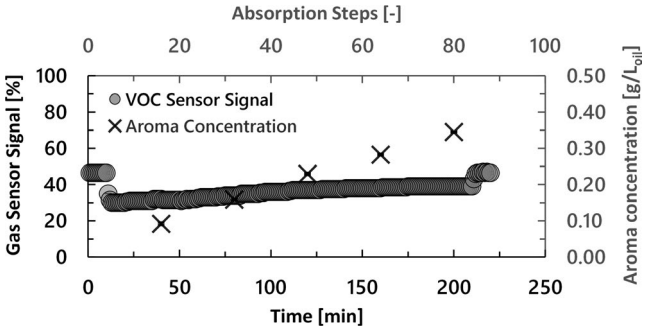

FIGURE 7 Time evolution of the gas sensor signal and liquid aroma concentration for the absorption of benzaldehyde in an RPB with the recycle of rapeseed oil (G = 100 L/min; L = 1 L/min; L_tot = 2.5 L; ω = 2750 rpm; N = 2)

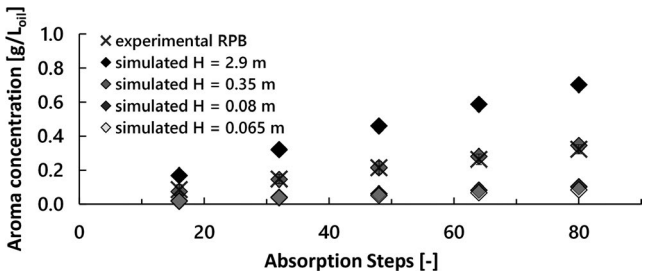

FIGURE 8 Comparison of the liquid aroma concentration during the absorption of benzaldehyde in rapeseed oil with the recycle of liquid phase for RPB and packed column

entire time of the experiment. Thus, the gaseous aroma concentration in the RPB outlet is always lower compared to the inlet causing lower VOC signal. However, as the recycled liquid phase becomes more loaded with aroma, the driving force for mass transfer decreases, causing less aroma being absorbed from the gaseous phase with proceeding time of the experiment, and thus, higher off-gas concentrations detected. With the large initial amount of recycled oil and low gaseous aroma concentration used in this experimental set-up, no full saturation of the rapeseed oil and, as a result, no absorption steady state were reached here. The measurements of the liquid phase confirmed the constant enrichment of rapeseed oil with the aroma compound. After 80 absorption steps corresponding to 200 minutes of rapeseed oil recycle, a benzaldehyde concentration of 0.323 ± 0.026 g/L$_{oil}$ could be achieved.

For comparison purposes, the experimental performance of the RPB for the aroma absorption in the recycled rapeseed oil is compared with a simulated conventional packed column (Figure 8).

From Figure 8, it is evident that a column with a packed height of just H = 0.065 m equal to the radial depth of the packing used in RPB would deliver just around a fifth to a quarter of the oil phase enrichment achieved in the RPB. As such column provides slightly less surface area as determined for the RPB, a comparison with a column of H = 0.08 m delivering equal surface area seems more legit. Here, the often-cited mass transfer improving characteristics of the RPB becomes obvious as the enrichment of the oil phase achieved at equal surface area is 3 to 4 times larger in an RPB. In order to achieve the same performance as the RPB, the conventional column needs to be packed with H = 0.35 m operating with 4.3 times larger surface area. Thus, the use of RPB leads to an intensified process with less mass transfer area needed for equal separation efficiency. However, a relatively small column with just H = 2.9 m of packing would deliver about more than a double aroma loading in the oil phase, increasing the space-time yield of the process. These results make clear that the RPB used outperforms the conventional absorption columns at similar dimensions by an increased mass transfer. The rotation supported process intensification makes it possible to get equal performance at a reduced surface area. However, for a recovery optimized aroma absorption, the laboratory-scale RPB used in this study significantly lacks mass transfer area. Although the laboratory-scale RPB used does not seem preferable over small packed columns, one of its advantages is the fact that the rotation supported liquid distribution and a film flow along the spirals of the packing used allow the processing of highly viscous liquids like plant oils at only moderate viscosity induced pressure drop increase.

3.1 | Investigation of pressure drop dependence on absorbent's viscosity

In order to prove that the pressure drop in a rotating packed bed does not reach uneconomically high levels when using oil as an absorbent, the viscosity of the liquid was varied between 1 and 100 mPa·s. Results of the wet pressure drop measurements and simulations in a packed column are displayed in Figure 9.

The pressure drop rises only slightly with increased viscosity for all gas load factors tested, and the measured effect is even stronger for higher gas load factors. At lower gas load factors, the viscosity effect lies within the measurement precision of $\Delta p = \pm 10$ Pa even at the highest viscosities tested and can be neglected. At the highest gas load factor, a slight increase in the pressure drop could be observed for the viscosities larger than 50 mPa·s only. As the distribution of such viscous absorbents could be challenging in a conventional laboratory-scale packed column, the pressure drop was simulated. The column's diameter was set to give an equal gas load factor at an equal gas flow rate as in an RPB. The pressure drop in

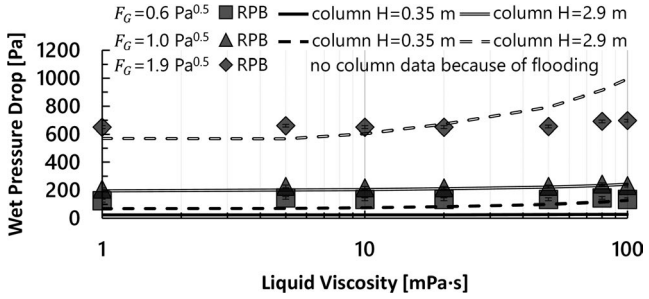

FIGURE 9 Wet pressure drop of an RPB (measured) and of a packed column (simulated) for different liquid viscosities at different gas load factors (L = 1.5 L/min; ω = 1500 rpm; N = 2; error bars based on measurement precision of $\Delta p = \pm 10$ Pa)

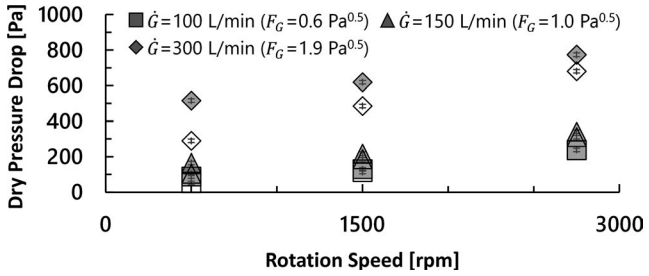

FIGURE 10 Dry pressure drop of an RPB measure for different rotation speed at different gas flow rates (open symbols: no packing included; solid symbols: spiral packing included; N = 2; error bars based on measurement precision of $\Delta p = \pm 10$ Pa)

an equally performing column of just 0.35 m height was at low gas load factors lower than in the RPB regardless of the liquid viscosity. However, for the highest gas load factor, no pressure drop could be simulated for the column because flooding occurred even with low liquid viscosity. As the pressure drop is proportional to the packing height, it is obvious that a column of 2.9 m height had a much larger pressure drop at equal gas load factors than an RPB. According to the simulation, such column exceeded 80% flooding boundary already at the F_G = 1.0 Pa$^{0.5}$, and at F_G = 1.9 Pa$^{0.5}$ no meaningful results could be generated as flooding exceeded 200%, and the pressure drop calculated was larger than 2 bar. Here, the effect of the absorbent viscosity became visible as the pressure drop of this packed column increased stronger than in an RPB, starting already at 5 mPa s which would make experimental investigations difficult indeed.

Unlike in packed columns, in the RPB the liquid, forced to flow as a thin wall film by the structure of the spiral packing and the rotation applied, does not present an additional resistance for the gas flow to overcome. The main pressure drop is generated by the gas inlets and outlets as well as by the rotation. To prove the hypothesis, dry pressure drop measurements are performed (Figure 10). Obviously, the gas flow rate is the dominating factor influencing the pressure drop. Besides the gas flow rate, the applied rotation is one of the main causes for pressure drop as with the increased rotation, the slip between the rotor and the incoming gas increases. Despite the expectations, the less porous spiral packing does not cause much additional pressure drop. At low gas flow rates, the data point of the measurements with packing and without packing overlaps. The packing effect could be observed reliably once again only at the largest gas flow rate tested.

The results of the pressure drop experiments emphasize the advantage of the rotation supported liquid distribution in an RPB for processing highly viscous liquids like plant oils. Although the current machine design and the rotation lead to a larger pressure drop in an RPB compared to packed columns at low gas load factors, the minor viscosity induced pressure drop increase enables a wider operational window, a more stable process and lower costs for the gas transport making RPBs beneficial for the use with plant oils at larger gas load factors.

3.2 | Estimation of the cavity zone effect

Despite the fact that the spiral packing design used in this study is obviously beneficial for the distribution of viscous absorbents, the low surface area generated on the spiral wall only does limit the mass transfer. The liquid surface area in the spiral packing should remain constant regardless of the liquid flow rate. Once the wall flow is established, and the entire spiral channel is wetted, the surplus of the absorbent will lead to an increasing film thickness only. In order to investigate this effect, the absorption of the lowest volatile aroma benzaldehyde was performed at different rapeseed oil flow rates (Figure 11). Besides, a comparison to an empty RPB, containing a rotor without any packing, allows an estimate of the cavity zone effect only. There are several reports published describing the cavity zone effect indicating that even when the packing is removed from the RPB, the casing still contributes significantly to the overall mass transfer.[40,41]

It is amazing that even without the packing high absorption efficiencies could be achieved. At each liquid throughput tested, the casing contributed on average roughly 67%-87% to the total absorption. The casing contribution to the overall absorption increased at larger flow rates and remained constant from 1 to 2 L/min once the liquid was fed in surplus. When the packing is removed from the rotor, the oil distributed from the open pipe axial to the rotor forms a film flow covering the bottom and the wall of the rotor bowl. This oil film breaks into droplets at the edges of the perforated rotor, and

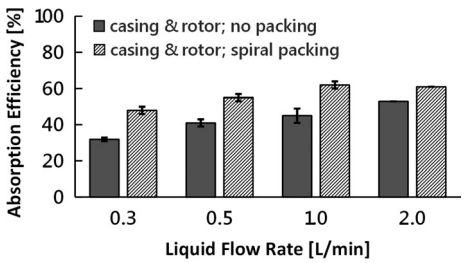

FIGURE 11 Dependency of the absorption efficiency on liquid flow rate for the absorption of benzaldehyde in rapeseed oil for the operation of the RPB without packing and with spiral packing ($\dot{G}$ = 100 L/min; ω = 2750 rpm; N = 3)

the spray formed in the gap between the rotor and the casing covers casing's wall and bottom. At high rotation speed and large liquid flow rates, the oil film was observed even at the top covers of both the casing and the rotor bowl after dismounting the machine. The high viscosity of the rapeseed oil used supports the coalescence of the droplets generated in the cavity zone into thin films on the casing wall, which presents an additional mass transfer area and increases the absorption. The total wetted surface area of the casing and the rotor without the packing is estimated in the range of 69%-88% of the surface area generated in the RPB when the packing is used.[1] Thus, once the casing is fully wetted at larger liquid flow rates and higher rotation speeds, it seems to contribute to the overall mass transfer according to the provided surface area. These observations make evident that especially in small laboratory-scale apparatuses like the RPB used in this study, the cavity zone effect is expected to be more severe than in larger RPB's where the larger packing generates much more mass transfer area than the casing. The scale-down of RPB comes with a significant shift in the proportion of mass transfer contribution from the packing towards the casing, which cannot be neglected when scaling up from laboratory to an industrial scale.

4 | CONCLUSIONS

The consumers' demand for all-natural formulations leads to an increasing interest in biotechnological aroma production. An absorption from gaseous process streams in a rotating packed bed is an innovative approach for downstream processing of biotechnological aromas. This study shows that the use of a centrifugal force inside a rotating spiral packing of an RPB leads to the formation of thin films, which decreases the mass transfer resistance and increases aroma absorption in viscous rapeseed oil. In an RPB, the rotation presents an additional degree of freedom and therefore allows processing of differently volatile molecules using the same equipment. Such flexibility poses a significant advantage over conventional packed columns. Thus, the process intensification in a high gravity field allows to outperform conventional packed columns at equal packing dimensions. Altogether, these results demonstrate the advantages of RPB application for the recovery of biotechnologically produced aromas. An additional benefit of the RPB compared to conventional columns is the fact that the rotation supported liquid distribution makes it possible to process highly viscous liquids such as plant oil at minor pressure drop increase. Whenever viscous plant oils are used as an absorbent for the recovery of aroma compounds and concerns about liquid distribution in static packed columns exist, the application of RPB technology should be considered as a method for process intensification. However, a compact design of an RPB combined with the spiral packing of limited dimensions limits the available mass transfer area. As the simulated columns were relatively small compared to the ones usually used in the industry, an often reported benefit of space savings in an RPB is questionable for this particular application. The RPB use remains thus restricted to special cases only when a packed column comes to its operability limits. For the industrial-scale processes, the RPB technology might find its application within the biotechnological downstream in cases of space limitations. When the high of the planned apparatus is restricted during the retrofit or, for example, in a container plant, the RPB seems a suitable replacement for the static packed column. The advantages of compact equipment seem in any case subordinate to the technically better performance for the biotechnological processes. Besides, most of the surface area available for the mass transfer and by that most of the achieved performance in the current laboratory-scale machine origins from the casing and the rotor showing the hurdle of equipment scale up and down. All in all, these results show that the RPB presents a suitable alternative for the recovery of biochemically produced aromas from gaseous process streams. Especially when the use of plant-based absorbents is beneficial, but the handling of high viscosity might be challenging in the packed columns, the RPB should be considered as an opportunity for process intensification. This particular benefit of RPB might also be advantageous for industrial-scale biofuel production with its viscous oil feeds and glycerol by-product. However, the small packing volume and the relatively low pressure drops presented in this laboratory-scale study do not have comparative significance for large-scale industrial processes. The evaluation of the RPB use for the intensification of biotechnological downstream processes would benefit from a comparison based on a relevant parameter like, for example, process costs. Also, the usual claims of space and costs savings originating from an intensified equipment need proper economic evaluation for biotechnological applications. Besides, the mass transfer phenomena in small-scale apparatuses and the scale-up rules need to be investigated more deeply. The experimentally measured data on thermodynamic aroma partitioning between real bioreactor off-gas and rapeseed oil would strongly improve the quality of the simulation and, by that, the significance of the comparisons drawn.

NOMENCLATURE

a	mass transfer area	[m^2]
$c^g_{aroma,in}$	gaseous aroma concentration in the inlet stream	[g_{aroma}/L_{air}]
$c^g_{aroma,out}$	gaseous aroma concentration in the outlet stream	[g_{aroma}/L_{air}]
Δc_i	concentration difference of a target compound	[mol/m^3]
D_{AB}	binary diffusion coefficient	[cm^2/s]
d_i	inner diameter of the packing used in RPB	[m]
d_o	outer diameter of the packing used in RPB	[m]
d_c	diameter of the packing used in simulated column	[m]
E	absorption efficiency	[%]

a	mass transfer area	[m^2]
F_G	gas load factor	[$Pa^{0.5}$]
$\dot{G}$	gas flow rate	[L/min]
g	gravitational acceleration	[m/s^2]
h	height of the packing used in RPB	[m]
Δh	height difference of the U-pipe manometer	[m]
H	height of the packing used in simulated column	[m]
H^{pc}	Henry's law coefficient	[Pa^*m^3/mol]
k	mass transfer coefficient	[1/s]
L_{tot}	absorbent volume	[L]
$\dot{L}$	liquid flow rate	[L/min]
N	number of experimental replications	[-]
$\dot{n}_i$	molar flow of a component	[mol/s]
η	viscosity	[mPa·s]
Δp	pressure drop	[Pa]
ρ	density	[kg/m^3]
S_{in}	gas sensor value of the inlet stream	[%]
S_{out}	gas sensor value of the out stream	[%]
S_0	gas sensor baseline value	[%]
δ	boundary layer thickness	[m]
ω	rotation speed	[rpm]

ACKNOWLEDGEMENT

The researcher group thanks M.Sc. Konrad Gładyszewski, Laboratory of Fluid Separations, Department of Biochemical and Chemical Engineering, TU Dortmund University, for the design and printing of the spiral packing used in this research. Open access funding enabled and organized by Projekt DEAL.

CONFLICT OF INTEREST

The author(s) have no conflict of interest in relation to this work.

ORCID

Ilya Lukin https://orcid.org/0000-0003-3901-2052

ENDNOTE

[1] The area of the generated spay was calculated under the assumptions found in Sang at al[41] and is one to two orders of magnitude lower than the casing area and thus can be neglected; especially, it is expected to remain equal for both configurations with and without packing.

REFERENCES

1. Leffingwell & Associates. 2013–2017 Flavor & Fragrance Industry Leaders. 2018. Available at: http://www.leffingwell.com/top_10.htm. Accessed October 1, 2018
2. Berger RG. Biotechnology of flavours - the next generation. *Biotechnol Lett*. 2009;31(11):1651-1659.
3. Cheetham PSJ. Combining the technical push and the business pull for natural flavours. In: Berger RG, ed. *Biotechnology of aroma compounds. Advances in biochemical engineering biotechnology*, 1st edn. Berlin Heidelberg New York: Springer; 1997:1-49.
4. Sales A, Paulino BN, Pastore GM, Bicas JL. Biogeneration of aroma compounds. *Curr Opin Food Sci*. 2018;19:77-84.
5. Serra S, Fuganti C, Brenna E. Biocatalytic preparation of natural flavours and fragrances. *Trends Biotechnol*. 2005;23(4):193-198.
6. Cataldo VF, López J, Cárcamo M, Agosin E. Chemical vs. biotechnological synthesis of C_{13}-apocarotenoids: Current methods, applications and perspectives. *Appl Microbiol Biotechnol*. 2016;100(13):5703-5718.
7. Bicas JL, Silva JC, Dionísio AP, Pastore GM. Biotechnological production of bioflavors and functional sugars. *Cienc Tecnol Aliment*. 2010;30(1):7-18.
8. Lukin I, Merz J, Schembecker G. Techniques for the recovery of volatile aroma compounds from biochemical broth: A review. *Flavour Fragrance J*. 2018;33(3):203-216.
9. Ramshew C, Mallinson RH, inventors; Imperial Chemical Industries Limited. Mass transfer process. U.S.A. 4,283,255. Aug. 11.
10. Zhao H, Shao L, Chen J-F. High-gravity process intensification technology and application. *Chem Eng J*. 2010;156(3):588-593.
11. Neumann K, Gładyszewski K, Groß K, et al. A guide on the industrial application of rotating packed beds. *Chem Eng Res Des*. 2018;134:443-462.
12. Wang Z, Yang T, Liu Z, Wang S, Gao Y, Wu M. Mass transfer in a Rotating Packed Bed: A critical review. *Chem Eng Process*. 2019;139:78-94.
13. Neumann K, Hunold S, Groß K, Górak A. Experimental investigations on the upper operating limit in rotating packed beds. *Chem Eng Process*. 2017;121:240-247.
14. Ramshaw C. HiGee distillation-an example of process intensification. *Chem Eng*. 1983;13-14.
15. Agarwal L, Pavani V, Rao DP, Kaistha N. Process intensification in higee absorption and distillation: design procedure and applications. *Ind Eng Chem Res*. 2010;49(20):10046-10058.
16. Rao DP, Bhowal A, Goswami PS. Process intensification in rotating packed beds (HiGee): An appraisal. *Ind Eng Chem Res*. 2004;43(4):1150-1162.
17. Sattler K. *Thermische Trennverfahren: 3. Absorption*, 3rd edn. Weinheim, New York, Chichester, Brisbane, Singapore, Toronto: Wiley-VCH; 2001.
18. Heymes F, Manno Demoustier P, Charbit F, Louis Fanlo J, Moulin P. Hydrodynamics and mass transfer in a packed column: Case of toluene absorption with a viscous absorbent. *Chem Eng Sci*. 2006;61(15):5094-5106.
19. Chamchan N, Chang J-Y, Hsu H-C, et al. Comparison of rotating packed bed and packed bed absorber in pilot plant and model simulation for CO_2 capture. *J Taiwan Inst Chem Eng*. 2017;73:20-26.
20. Guo K, Wen J, Zhao Y, et al. Optimal packing of a Rotating Packed Bed for H_2S removal. *Environ Sci Technol*. 2014;48(12):6844-6849.
21. Joel AS, Wang M, Ramshaw C, Oko E. Modelling, simulation and analysis of intensified regenerator for solvent based carbon capture using rotating packed bed technology. *Appl Energy*. 2017;203:11-25.
22. Jassim MS, Rochelle G, Eimer D, Ramshaw C. Carbon dioxide absorption and desorption in aqueous monoethanolamine solutions in a Rotating Packed Bed. *Ind Eng Chem Res*. 2007;46(9):2823-2833.
23. Thiels M, Wong DSH, Yu C-H, Kang J-L, Jang SS, Tan C-S. Modelling and design of carbon dioxide absorption in Rotating Packed Bed and packed column. *IFAC-PapersOnLine*. 2016;49(7):895-900.

24. Cheng H-H, Lai C-C, Tan C-S. Thermal regeneration of alkanolamine solutions in a rotating packed bed. *Int J Greenhouse Gas Control*. 2013;16:206-216.
25. Chiang C-Y, Lee D-W, Liu H-S. Carbon dioxide capture by sodium hydroxide-glycerol aqueous solution in a rotating packed bed. *J Taiwan Inst Chem Eng*. 2017;72:29-36.
26. Chiang C-Y, Liu Y-Y, Chen Y-S, Liu H-S. Absorption of hydrophobic volatile organic compounds by a rotating packed Bed. *Ind Eng Chem Res*. 2012;51(27):9441-9445.
27. Deutsche Gesellschaft für Fettwissenschaft e.V. Fettsäurezusammensetzung wichtiger pflanzlicher und tierischer-Speisefette und -öle. Available at: http://www.dgfett.de/material/fszus.php. Accessed August 7th 2019
28. Sander R. Compilation of Henry's law constants (version 4.0) for water as solvent. *Atmos Chem Phys*. 2015;15(8):4399-4981.
29. MacInnes JM, Zambri MKS. Hydrodynamic characteristics of a rotating spiral fluid-phase contactor. *Chem Eng Sci*. 2015;126:427-439.
30. Burns JR, Ramshaw C. Process intensification: Visual study of liquid maldistribution in rotating packed beds. *Chem Eng Sci*. 1996;51(8):1347-1352.
31. Lewis WK, Whitman WG. Principles of gas absorption. *Ind Eng Chem*. 1924;16(12):1215-1220.
32. Higbie R. The rate of absorption of a pure gas into a still liquid during short period of exposure. *Transaction of the AiChE*. 1935;31:365-389.
33. Formlabs. Material data sheet - Standard resin. 2019. Available at: https://formlabs-media.formlabs.com/datasheets/Standard-DataSheet.pdf. Accessed Accessed October 25, 2019
34. Thomas RG. Volatilization from water. In: Lyman WJ, Reehl WF, Rosenblatt DH, eds. *Handbook of chemical property estimation methods: Environmental behavior of organic compounds*. New York: McGraw-Hill; 1982:15–1-15–34.
35. Hanley B, Chen C-C. New mass-transfer correlations for packed towers. *AIChE J*. 2012;58(1):132-152.
36. Friedt W, Snowdon R. Oilseed rape. In: Vollmann J, Rajcan I, eds. *Oil Crops. First*. New York, NY: Springer-Verlag, New York; 2009:90-121. Handbook of Plant Breeding; 4.
37. Glycerine Producers' Association. *Physical properties of glycerine and its solutions*, 1st edn. New York: Glycerine Producers' Association; 1963.
38. Hottel HC, Noble JJ, Sarofim AF, Silcox GD, Wankat PC, Knaebel KS. Heat and mass transfer. In: Perry RH, Green DW, eds. *Perry's chemical engineers' handbook*, 8th edn. New York, NY: McGraw-Hill; 2008:5–1-5–83.
39. Holley ER. Diffusion and boundary layer concepts in aeration through liquid surfaces. *Water Res*. 1973;7(4):559-573.
40. Yang K, Chu G, Zou H, Sun B, Shao L, Chen J-F. Determination of the effective interfacial area in rotating packed bed. *Chem Eng J*. 2011;168(3):1377-1382.
41. Sang L, Luo Y, Chu G-W, Zhang J-P, Xiang Y, Chen J-F. Liquid flow pattern transition, droplet diameter and size distribution in the cavity zone of a rotating packed bed: A visual study. *Chem Eng Sci*. 2017;158:429-438.

How to cite this article: Lukin I, Pietzka L, Wingartz I, Schembecker G. Aroma absorption in rapeseed oil using rotating packed bed. *Flavour Fragr J*. 2021;36:137–147. https://doi.org/10.1002/ffj.3623